Evidence of Lateral Nanoscale Heterogeneities in Weak Polyelectrolyte Brushes

Kevin N. Witte,† Jaehyun Hur,† Wei Sun, Sangtae Kim, and You-Yeon Won*

School of Chemical Engineering, Purdue University, West Lafayette, Indiana 47907

Received June 24, 2008
Revised Manuscript Received August 23, 2008

Polymeric brushes provide an intriguing way of creating "smart" surfaces whose properties can be tuned by external stimuli.[1] Of particular interest are weak polyelectrolytes because their degree of charging is governed by an acid−base equilibrium that can be spatially variant. Thus, the charge properties and chain conformations are responsive to changes in the pH, ionic strength, or temperature of the bulk solvent.[2−4] Recently, Szleifer and coworkers demonstrated, using a single-chain mean-field theory (SCMF), that due to the interplay of charge regulation, (poor) solvent quality, and salt effects, a single-component weak polyelectrolyte brush can become thermodynamically unstable with variations in the grafting density but also show increasing stability at higher ionic strengths (cf. Figure 1 of ref 5). For brushes where the grafting points are fixed, the phase separation would of necessity be microscopic in scale. However, if the grafting points were mobile along the surface, such as amphiphilic diblock copolymers at an interface or self-assembled in vesicular structures, the nature of the separation could be more long-ranged, leading to regions high in grafting density and regions of low grafting density. In this Communication we present, for the first time, experimental evidence, from amphiphilic diblock copolymers adsorbed as a Langmuir monolayer at the air−water interface, of thermodynamic instability, resulting in phase separation of a single-component polyelectrolyte brush with mobile grafting points. Further, this behavior is shown, by AFM imaging of Langmuir−Blodgett depositions on a solid hydrophobic substrate, to be long-range "frustrated", leading to a microscopic phase separation which can be eliminated upon the addition of large quantities of monovalent salt.

Amphiphilic diblock copolymers adsorbed to the air−water interface are known, in many cases, to be poor model systems of true brush systems. Some systems, particularly those that utilize polystyrene (PS) as an anchoring block, form micelle-type structures on the water surface.[6−8] The existence of these micelles renders the system unsuitable for use as a model brush system as the hydrophilic grafting points are not uniformly distributed. Further, block copolymer films with low hydrophobic content can become corrugated at high surface pressures.[9] Also, many polymers, including poly(ethylene oxide) (PEO),[10−12] sulfonated PS (PSS),[13] and poly(2-(dimethylamino)ethyl methacrylate) (PDMAEMA),[14] are known to adsorb strongly to the interface at low surface coverage in order to minimize the interfacial energy due to the high surface tension between air and water. All of these issues would result in nonsmooth surfaces of the adsorbed layer. Judicious choice of the anchoring block, however, can eliminate these concerns.

In this work, a diblock copolymer is used where the soluble block is PDMAEMA, a tertiary amine polymer, with monomer pK_a of 8.4,[15] whose backbone chain is hydrophobic, and the anchoring block is poly(*n*-butyl acrylate) (PnBA). This PDMAEMA−PnBA copolymer was synthesized by atom transfer radical polymerization (ATRP), and each block has a number-average degree of polymerization ($\overline{DP}_n$) of 80 and 94, respectively, as characterized by ^{1}H NMR, and a polydispersity index (PDI) of 1.31, as determined by GPC (see section S1 of the Supporting Information (SI) for greater detail). The choice of PnBA as the hydrophobic anchoring block prevents many of the issues discussed above that are normally associated with polymers spread at the air−water interface. The tendency of a hydrophobic polymer to create surface micelles can be considered in terms of the spreading coefficient defined as $S \equiv \gamma_{\text{air-water}} - (\gamma_{\text{polymer-air}} + \gamma_{\text{polymer-water}})$,[16] where γ_{a-b} denotes the surface/interfacial tension between phases a and b (e.g., $\gamma_{\text{air-water}} = 73$ mJ/m^2 at 20 °C[17]). Polymers that dewet from the water surface and form surface micelles have negative values of the spreading coefficient (e.g., for PS at 20 °C, $\gamma_{\text{PS-air}} = 40$ mJ/m^2 [18] and $\gamma_{\text{PS-water}} = 41$ mJ/m^2,[17] which gives $s = -8$ mJ/m^2 at the given temperature). Conversely, polymers that wet the water surface and form uniform monolayers should have positive values (e.g., for PnBA at 20 °C, $\gamma_{\text{PnBA-air}} = 33$ mJ/m^2 [18] and $\gamma_{\text{PnBA-water}} = 19.6 \pm 4.9$ mJ/m^2 (measured in this study as described in section S2 of the SI), which gives $s = 21$ mJ/m^2 at the given temperature). This uniform surface coverage and low surface energy will ensure that the PDMAEMA chains prefer to be in the brush state as opposed to adsorbing to the surface at relatively low grafting densities. In addition, PnBA has a spreading coefficient of $s = 7.8$ mJ/m^2 at 20 °C at the graphite−water interface as calculated from contact angle measurements made in air (see section S2 in the SI) and the graphite−water contact angle of 86°.[19] Another advantage of PnBA as an anchoring block is its low glass transition temperature, $T_g = -55$ °C.[20] The nonglassy nature of the polymer allows it to relax on a reasonable time scale as compared to glassy polymers. This may be why no corrugation of PnBA monolayers at the air−water interface was observed even at high surface coverage (supporting data presented in section S3 of the SI).

The ability of a PnBA anchoring block to form a uniform monolayer at the air−water interface which can be reliably transferred onto a graphite substrate immersed in water was confirmed by studying the behavior of PnBA homopolymer at the corresponding interfaces. Figure 1a shows a representative pressure−area isotherm for a PnBA polymer ($\overline{DP}_n = 111$ and PDI = 1.12) measured at the air−water interface on a KSV 5000 Langmuir trough (see section S4 of the SI for details); the isotherm was reproducible in the x-direction within ±2% among three independent measurements with almost negligible errors in the pressure values. Beginning at high area per chain the classic ideal gas-type behavior is observed. As the compression commences the isolated coils begin to collide with greater frequency, leading to a steep rise in the surface pressure. The x-intercept of the extrapolated line of the steepest section of the isotherm is estimated to be $A = 3206 \pm 107$ Å^2/chain, which gives a monolayer thickness of about 8.3 ± 0.3 Å at the onset of the steep pressure rise, confirming that PnBA indeed completely wets and forms a spread film on the water surface. This pressure rise, we believe, continues until the surface is completely covered by a uniform monolayer. At this point, about 2390 ± 82 Å^2/chain, a sharp transition occurs to a plateau where

* To whom correspondence should be addressed. E-mail: yywon@ecn.purdue.edu.
† Authors with equal contributions.

10.1021/ma801412u CCC: $40.75 © 2008 American Chemical Society
Published on Web 11/04/2008

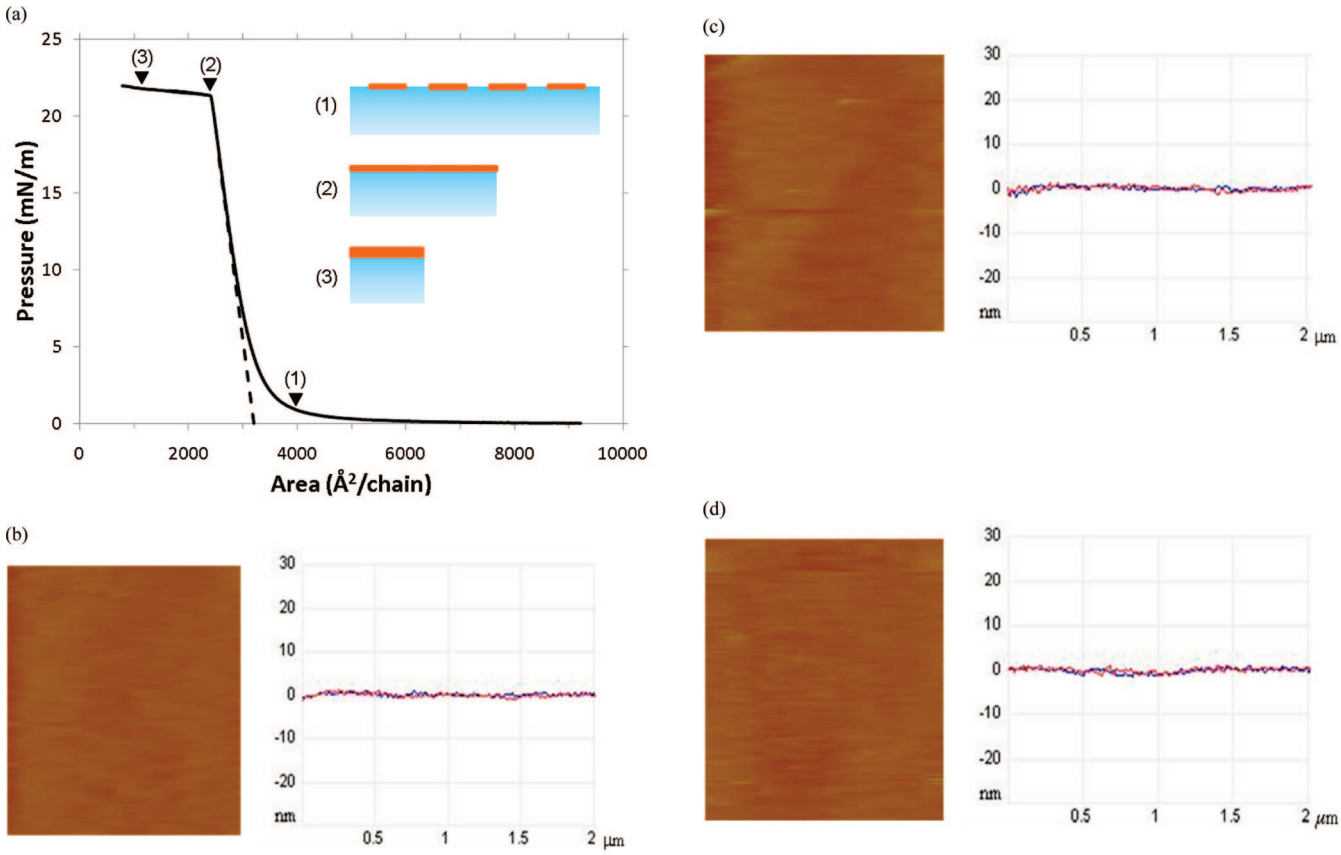

Figure 1. Results for PnBA with $\overline{DP}_n = 111$. (a) Surface pressure−area isotherm showing characteristic plateau at $A = 2390$ Å^2/chain. Dotted line represents linear extrapolation from the point of greatest slope to area per chain where overlap occurs. Cartoons illustrate the expected configurations of the PnBA polymers on the water surface. Representative fluid AFM tapping-mode height images (2 μm × 2 μm) and topography scans (along arbitrary horizontal (blue) and vertical (red) lines) taken for films deposited at (b) 5000, (c) 3000, and (d) 1500 Å^2/chain.

the monolayer is expected to begin forming a multilayer structure. The pressure at this point is $\pi = 21.3 \pm 0.2$ mN/m, which leads to a calculated interfacial tension between the polymer and water phases of $\gamma_{PnBA-water} = \gamma_{air-water} - \gamma_{PnBA-air} - \pi = 18.7 \pm 2.2$ mN/m, which is in excellent agreement with the value determined from contact angle measurements (i.e., 19.6 ± 4.9 mJ/m^2). This point also gives an estimate for the mean monomer area of 22 ± 1 Å^2, which is in good agreement with estimates of 23 Å^2 for poly(*tert*-butyl methacrylate) (PtBMA)[21] and 20−21 Å^2 for poly(isobutyl methacrylate) (PiBMA).[22] This data all support that the PnBA is forming a uniform continuous film in the plateau regime. Here the water surface is completely coated with PnBA, and due to the liquidlike nature of the polymer film, no stress is stored in the interface during the compression, giving rise to a flat surface pressure; the exact nature of this plateau and the conformational properties of the polymers in this regime are currently under thorough investigation and are beyond the scope of the present paper. Further compression through the plateau region did not produce a second upturn of the pressure−area isotherm within the area-per-chain measurement window, although such behavior has been reported for a similar polymer, PtBMA;[21] we suspect that this second rise in the pressure at high compression is related to the glassy nature of the polymers studied. At 5000, 3000, and 1500 Å^2/chain, LB depositions were made. Briefly, a graphite substrate was lowered into the subphase using a Kibron minitrough at a speed of 1 mm/min, holding the surface pressure constant. A 100% monolayer-transfer efficiency is expected due to the lack of viscous drag at the contact line that is seen in the lifting case.[23] The resulting deposited film was kept submerged in the subphase and imaged using fluid AFM. The results are

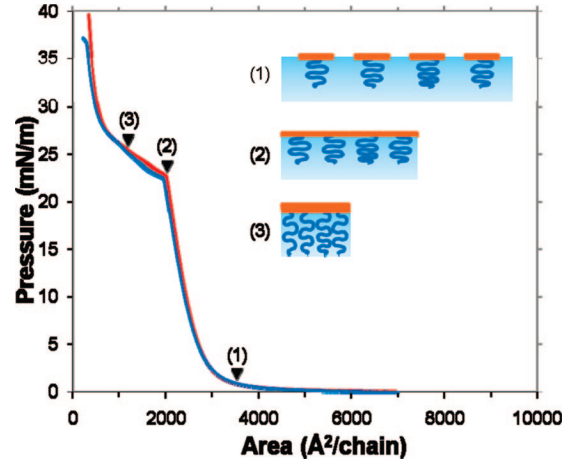

Figure 2. Surface pressure−area isotherm for PDMAEMA−PnBA with $\overline{DP}_n = 80$ and 94 for the PDMAEMA and PnBA blocks, respectively, at bulk NaCl concentrations of $C_{salt} = 0$ (red) and 100 mM (blue). Cartoons represent the expected brush configurations at the interface, illustrating the continuous film formation (at point 2) and the "mushroom to brush" transition (i.e., state 2 → state 3).

shown in Figure 1b−d where only a smooth surface is visible in the tapping-mode height images. Thus, taken together, the conclusion is that a smooth uniform PnBA anchoring layer is created at the air−water interface.

Since PnBA forms a uniform anchoring layer, the structure and behavior of the PDMAEMA polyelectrolyte brushes can be studied as a model polyelectrolyte brush system. Figure 2 shows the pressure−area isotherms for the PDMAEMA−PnBA diblock copolymer under neutral pH conditions for two concentrations

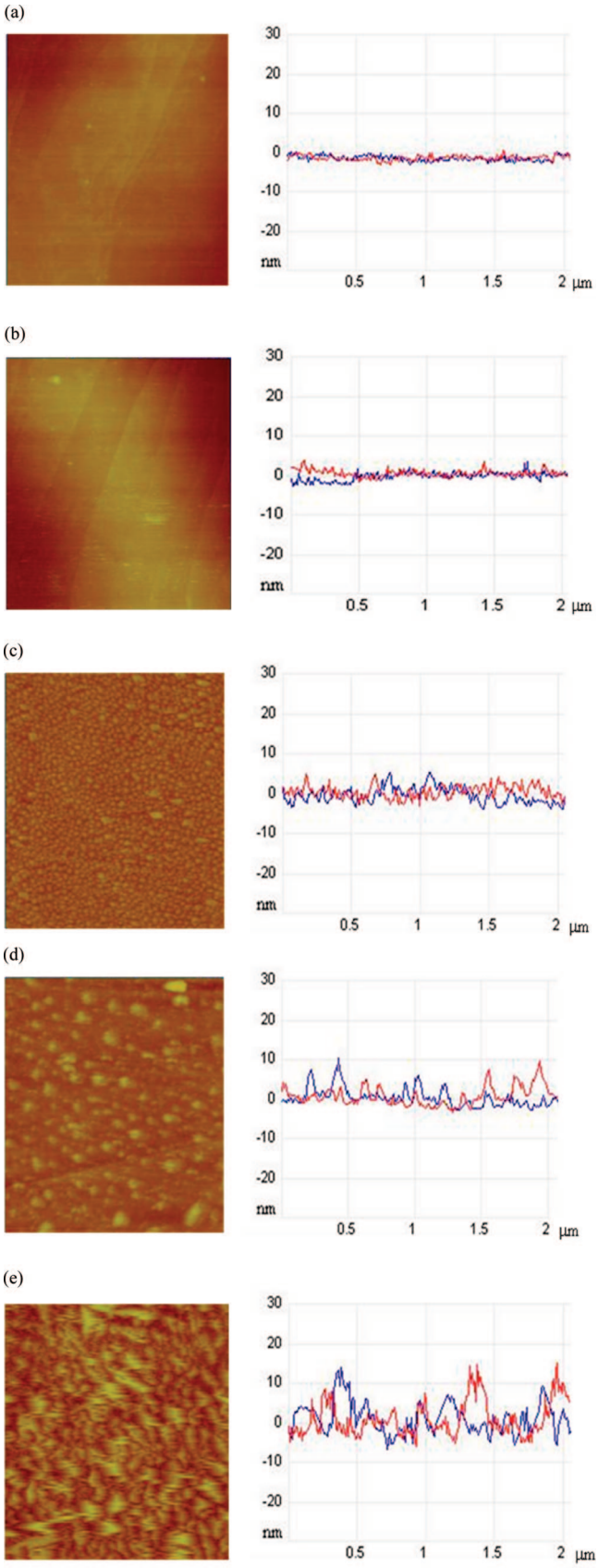

Figure 3. Representative fluid AFM tapping-mode height images (2 μm × 2 μm) and topography scans (along arbitrary horizontal (blue) and vertical (red) lines) for PDMAEMA−PnBA ($\overline{DP}_n$ = 80 and 94 for the PDMAEMA and PnBA blocks, respectively) deposited at (a) 3887, (b) 2591, (c) 1943, (d) 1296, and (e) 648 Å^2/chain on graphite where the bulk NaCl concentration is 0 mM.

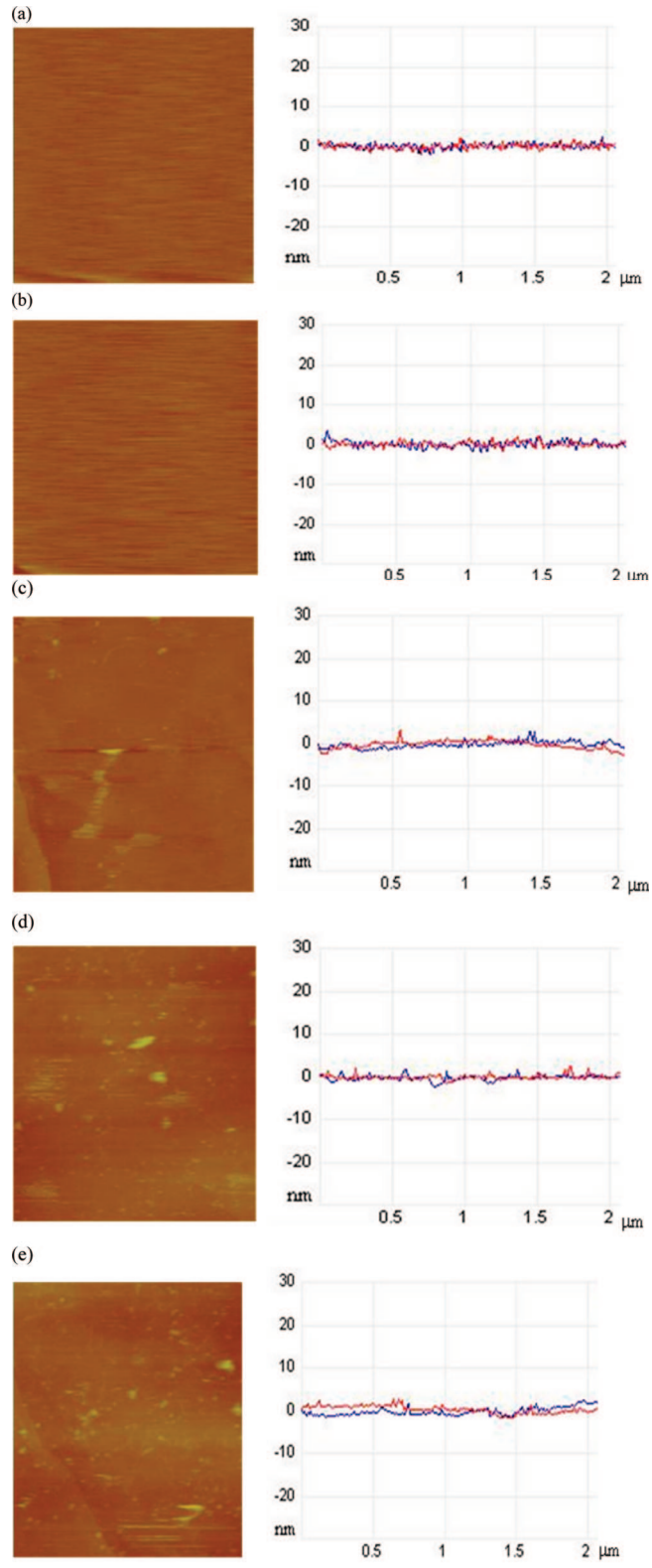

Figure 4. Fluid AFM tapping-mode height images (2 μm × 2 μm) and topography scans (along arbitrary horizontal (blue) and vertical (red) lines) for PDMAEMA-PnBA ($\overline{DP}_n$ = 80 and 94 for the PDMAEMA and PnBA blocks, respectively) deposited at (a) 3887, (b) 2591, (c) 1943, (d) 1296, and (e) 648 Å^2/chain on graphite where the bulk NaCl concentration is 100 mM.

of added NaCl: 0 and 100 mM. Both isotherms show the steep increase from onset until a sharp transition point around 2000 Å^2/chain which can be attributed mostly to the PnBA anchor block as it forms a continuous film layer. The zero salt case shows a slightly steeper slope during the initial pressure rise

probably due to the influence of the unscreened brush chains. After the transition point, however, the zero salt case shows a monotonic increase in the pressure while the salted brush shows a signature of the existence of another plateau followed by an initial secondary rise. Both systems then show a steep final pressure rise, the unsalted case having a steeper slope. The differences can be understood in terms of relative electrostatic interactions.

To understand the effects of these differing electrostatic interactions on the structure of the brush systems, the Langmuir monolayer of the PDMAEMA−PnBA diblock copolymer was LB-deposited on a graphite substrate (typically after a 5 min equilibration at the air−water interface at each given compression area), and the resultant brushes were imaged (within 24 h after the LB deposition) with fluid AFM as described above. Figure 3 shows the height mode results at 3887, 2591, 1943, 1296, and 648 Å^2/chain for the unsalted case. Clearly, near the onset of the continuous film formation of the PnBA chains, a marked inhomogeneity appears in the images; the appearance of the heterogeneities must occur between 2590 and 1940 Å^2/chain although the plateau transition is believed to only coincidently be in the same range. However, this range appears to coincide with the expected mushroom-to-brush transition which was minimally estimated by the de Gennes condition[24] for a fully screened Θ-solvent condition to be around 1589 Å^2/chain ($= \pi C_\infty n l^2/6$ where $n = 160$ in our case) using parameters for the similarly sized poly(*n*-butyl methacrylate) (i.e., $C_\infty = 8.0$ and $l = 1.54$ Å);[25] this is only a very minimal estimation, and the true transition is expected to be at a higher value of the area per chain. This means that all the observed behavior occurs within the brush regime. These inhomogeneities are believed to be domains rich in PDMAEMA which have been created due to the thermodynamic instability of the weak polyelectrolyte layer as recently predicted theoretically by Szleifer and co-workers.[5] Notice further that the domains are limited in size at a given pressure. To confirm the microscopic nature of the lateral phase-separated structure that develops upon compression, we examined the structure of the same brushes deposited on graphite but this time prepared with a longer equilibration time (i.e., 24 h) prior to the LB deposition. As shown in Figure S3 of the SI, this long equilibration time did not cause any detectable change in the sizes of the microphase-separated structures, indicating the absence of any time-dependent coalescence of the microdomains and thus the long-lasting (if not equilibrium) nature of the microphase-separated state. In section S8 of the SI, we also provide indirect evidence that once deposited on graphite, the PDMAEMA brush layer formed by the PDMAEAM−PnBA copolymer undergoes negligible structural relaxation or rearrangement, suggesting that the microphase separation behavior observed with the LB-deposited samples is representative of that of the original brushes constructed at the air−water interface.

If the existence and structure of these inhomogeneous domains are in fact regulated by electrostatic effects, then they are expected to disappear upon the addition of enough monovalent salt to screen the electrostatic interactions and stabilize the charged brush.[5,26] Figure 4 shows the AFM results taken at the same locations on the isotherm, but the subphase now contains 100 mM aqueous NaCl. Indeed, at all values of the area per chain, the inhomogeneities observed in the zero-salt case are greatly reduced in size and number. Certainly, the driving force for the formation of the observed inhomogeneities is greatly reduced upon the addition of salt to the subphase, in agreement with the predictions of Szleifer and co-workers.[5] However, the exact organization and makeup of the domains remain unclear and are the subject of ongoing study in our laboratory.

In this work, it has been demonstrated that a diblock copolymer can be used to study polymer brushes if the anchoring block spreads on the grafting interface and has nonglassy kinetics. Further, it was demonstrated that PDMAEMA brushes show thermodynamic instability and form heterogeneous regions of different brush heights. Also, the separation was observed to be long-range "frustrated" where the domains remained microscopic in scale at equilibrium. Finally, the addition of large amounts of salt was shown to prevent the formation of these domains confirming their electrostatic origin.

Acknowledgment. The authors are grateful for financial support of this research from the American Chemical Society Petroleum Research Fund (Grant 46593-G7), the 3M Company (Nontenured Faculty Award), and the Purdue Research Foundation Shreve Fund. We also express our deep gratitude to Dr. Jeffrey Youngblood and John Howarter for their assistance with the contact angle measurements.

Supporting Information Available: Experimental details. This material is available free of charge via the Internet at http://pubs.acs.org.

References and Notes

(1) Sidorenko, A.; Minko, S.; Schenk-Meuser, K.; Duschner, H.; Stamm, M. *Langmuir* **1999**, *15* (24), 8349–8355.
(2) Israels, R.; Leermakers, F. A. M.; Fleer, G. J. *Macromolecules* **1994**, *27* (11), 3087–3093.
(3) Borukhov, I.; Andelman, D.; Orland, H. *Eur. Phys. J. B* **1998**, *5* (4), 869–880.
(4) Ruhe, J.; Ballauff, M.; Biesalski, M.; Dziezok, P.; Grohn, F.; Johannsmann, D.; Houbenov, N.; Hugenberg, N.; Konradi, R.; Minko, S.; Motornov, M.; Netz, R. R.; Schmidt, M.; Seidel, C.; Stamm, M.; Stephan, T.; Usov, D.; Zhang, H. N. *Adv. Polym. Sci.* **2004**, *165*, 79–150.
(5) Gong, P.; Genzer, J.; Szleifer, I. *Phys. Rev. Lett.* **2007**, *98* (1).
(6) Chung, B.; Choi, M.; Ree, M.; Jung, J. C.; Zin, W. C.; Chang, T. H. *Macromolecules* **2006**, *39* (2), 684–689.
(7) Cox, J. K.; Yu, K.; Constantine, B.; Eisenberg, A.; Lennox, R. B. *Langmuir* **1999**, *15* (22), 7714–7718.
(8) Zhu, J. Y.; Eisenberg, A.; Lennox, R. B. *J. Am. Chem. Soc.* **1991**, *113* (15), 5583–5588.
(9) Dubreuil, F.; Guenoun, P. *Eur. Phys. J. E* **2001**, *5* (1), 59–64.
(10) Faure, M. C.; Bassereau, P.; Carignano, M. A.; Szleifer, I.; Gallot, Y.; Andelman, D. *Eur. Phys. J. B* **1998**, *3* (3), 365–375.
(11) Bijsterbosch, H. D.; Dehaan, V. O.; Degraaf, A. W.; Mellema, M.; Leermakers, F. A. M.; Stuart, M. A. C.; Vanwell, A. A. *Langmuir* **1995**, *11* (11), 4467–4473.
(12) Cao, B. H.; Kim, M. W. *Faraday Discuss.* **1994**, 245–252.
(13) Kaewsaiha, P.; Matsumoto, K.; Matsuoka, H. *Langmuir* **2004**, *20* (16), 6754–6761.
(14) Rehfeldt, F.; Steitz, R.; Armes, S. P.; Von Klitzing, R.; Gast, A. P.; Tanaka, M. *J. Phys. Chem. B* **2006**, *110* (18), 9171–9176.
(15) van de Wetering, P.; Zuidam, N. J.; van Steenbergen, M. J.; van der Houwen, O.; Underberg, W. J. M.; Hennink, W. E. *Macromolecules* **1998**, *31* (23), 8063–8068.
(16) Evans, D. F.; Wennerström, H. *The Colloidal Domain: Where Physics, Chemistry, Biology, and Technology Meet*; VCH Publishers: New York, 1994.
(17) Wu, S. *Polymer Interface and Adhesion*; Marcel Dekker: New York, 1982.
(18) Brandrup, J.; Immergut, E. H. *Polymer Handbook*, 3rd ed.; Wiley: New York, 1989.
(19) Fowkes, F. M.; Harkins, W. D. *J. Am. Chem. Soc.* **1940**, *62*, 3377–3386.
(20) Roff, W. J. *Handbook of Common Polymers: Fibres, Films, Plastics, and Rubbers*; CRC Press: Cleveland, 1971.
(21) Gavranovic, G. T.; Deutsch, J. M.; Fuller, G. G. *Macromolecules* **2005**, *38* (15), 6672–6679.
(22) Naito, K. *J. Colloid Interface Sci.* **1989**, *131* (1), 218–225.
(23) Hur, J.; Won, Y. Y. *Soft Matter* **2008**, *4* (6), 1261–1269.
(24) de Gennes, P. G. *Macromolecules* **1980**, *13* (5), 1069–1075.
(25) Aharoni, S. M. *Macromolecules* **1983**, *16* (11), 1722–1728.
(26) Witte, K. N.; Won, Y. Y. *Macromolecules* **2006**, *39* (22), 7757–7768.

MA801412U